Photoexcited electron dynamics and energy loss rate in silicon: temperature dependence and main scattering channels

Raja Sen, Nathalie Vast, Jelena Sjakste

Photoexcited electron dynamics and energy loss rate in silicon: temperature dependence and main scattering channels

R. Sen, N. Vast, J. Sjakste

Laboratoire des Solides Irradiés, CEA/DRF/IRAMIS, École Polytechnique, CNRS, Institut Polytechnique de Paris, 91120 Palaiseau, France

ABSTRACT

In this work, we revisit the DFT-based results for the electron-phonon scattering in highly excited silicon. Using state-of-the-art *ab initio* methods, we examine the main scattering channels which contribute to the total electron-phonon scattering rate and to the energy loss rate of photoexcited electrons in silicon as well as their temperature dependence. Both temperature dependence and the main scattering channels are shown to strongly differ for the total electron-phonon scattering rate and for the energy loss rate of photoexcited electrons. Whereas the total electron-phonon scattering rate increases strongly with temperature, the temperature dependence of the energy loss rate is negligible. Also, while acoustic phonons dominate the total electron-phonon scattering rate at 300 K, the main contribution to the energy loss rate comes from optical modes.

Keywords: electron-phonon coupling, semiconductor, photoexcited electrons, silicon

1. INTRODUCTION

Today, the computational methods based on the density functional theory, on the one hand,[1–3] and of the time-, energy-, and momentum-resolved spectroscopy, on the other hand,[4–9] provide an unprecedently detailed insight into the processes governing hot-electron relaxation dynamics, and, in particular, into the role of the electron-phonon coupling.

For photoexcited carriers, one can identify two distinct relaxation regimes, both determined by the electron-phonon scattering: one is related to the loss of the initial momentum (redistribution of carriers in the Brillouin zone), and the other to the energy transfer from electrons to phonons.[3,6] In some cases, the two-photon photoemission experiments were able to capture both the initial momentum randomization regime and the energy transfer regime: this was achieved, e.g. in Refs. 3, 6 for GaAs. However, for highly excited electrons, the relaxation times related to the loss of the initial momentum can be as fast as a few femtoseconds,[10,11] and often unmeasurable,[11,12] so that only the relaxation times related to the energy transfer from electrons to phonons can be measured experimentally. This was the case e.g. in Ref. 12 for silicon as well as for other materials such as InSe.[8,13]

In Ref. 12, the rate of energy transfer from electrons to phonons in silicon (referred to as the energy relaxation rate in Refs. 3, 6, 12, and energy loss rate in other works[14]) has been measured by two-photon photoemission experiment over a large range of photoexcited electron energies, at 300 K, and found in good agreement with DFT-based calculations.[12]

Here, we examine, using methods based on density functional theory (DFT), the temperature dependence and the main scattering channels of the energy loss rate of the photoexcited electrons in silicon, due to the electron-phonon scattering, and compare them to those of the total scattering rate. Provided that often, time-resolved spectroscopy provides only the insight into the energy transfer, it is important to keep in mind that some properties, such as temperature dependence and main scattering scattering channels, might not be the same for the total scattering rate and for the energy transfer rate, even if both rates are determined by the electron-phonon scattering.[3,14,15]

jelena.sjakste@polytechnique.edu

The paper is organized as follows: First, we will present briefly the technical details of our calculations, and remind the reader of the definition of the energy transfer rate from electrons to phonons. Then, we will present the DFT results for the temperature dependence of the energy transfer rate and for the main electron-phonon scattering channels which contribute to the energy transfer, and show them to be different from those of the total scattering rate.

2. THEORETICAL FRAMEWORK AND COMPUTATIONAL DETAILS

The total electron-phonon scattering rate, or self-energy, is implemented, e.g., in the EPW code[16] and defined in numerous other works:[3,17]

$$\tau_{n\mathbf{k}}^{-1} = \Gamma_{em} + \Gamma_{abs} \tag{1}$$

where

$$\begin{aligned}\Gamma_{em} &= \frac{2\pi}{\hbar}\Sigma_{m\nu}\int \frac{d\mathbf{q}}{\Omega_{BZ}}|g_{mn\nu}(\mathbf{k},\mathbf{q})|^2(N_{\mathbf{q},\nu}+1-f_{m,\mathbf{k+q}})\delta(\varepsilon_{n,\mathbf{k}}-\varepsilon_{m,\mathbf{k+q}}-\hbar\omega_{\mathbf{q}\nu})\\ \Gamma_{abs} &= \frac{2\pi}{\hbar}\Sigma_{m\nu}\int \frac{d\mathbf{q}}{\Omega_{BZ}}|g_{mn\nu}(\mathbf{k},\mathbf{q})|^2(N_{\mathbf{q},\nu}+f_{m,\mathbf{k+q}})\delta(\varepsilon_{n,\mathbf{k}}-\varepsilon_{m,\mathbf{k+q}}+\hbar\omega_{\mathbf{q}\nu})\end{aligned} \tag{2}$$

Here, all emission and absorption processes allowed by energy and momentum conservation are taken into account. $g_{mn\nu}(\mathbf{k},\mathbf{q})$ stand for the electron-phonon matrix elements between electronic states with m and n band numbers, coupled *via* the phonon mode ν. $N_{\mathbf{q},\nu}$ stand for phonon population numbers (Bose-Einstein distribution), $f_{n,\mathbf{k}}$ is the electron Fermi-Dirac distribution function, $\varepsilon_{n,\mathbf{k}}$ are electron eigenenergies and $\omega_{\mathbf{q}\nu}$ are phonon frequencies. The total electron-phonon scattering rate expresses the probability for an excited electron to change its initial momentum, i.e. to be scattered elsewhere in the Brillouin zone, it was referred to as "momentum scattering rate" in some of our previour works.[3,6,11]

The energy relaxation rate, or, equivalently, the rate of energy transfer to phonons, reads:[3,14,17]

$$\begin{aligned}\frac{\delta E}{\delta t} &= \Gamma_{em}\omega_{em} - \Gamma_{abs}\omega_{abs} = \\ \frac{2\pi}{\hbar}\Sigma_{m\nu}\int \frac{d\mathbf{q}}{\Omega_{BZ}}\omega_{\mathbf{q}\nu}|g_{mn\nu}(\mathbf{k},\mathbf{q})|^2(N_{\mathbf{q},\nu}+1-f_{m,\mathbf{k+q}})\delta(\varepsilon_{n,\mathbf{k}}-\varepsilon_{m,\mathbf{k+q}}-\hbar\omega_{\mathbf{q}\nu}) - \\ -\frac{2\pi}{\hbar}\Sigma_{m\nu}\int \frac{d\mathbf{q}}{\Omega_{BZ}}\omega_{\mathbf{q}\nu}|g_{mn\nu}(\mathbf{k},\mathbf{q})|^2(N_{\mathbf{q},\nu}+f_{m,\mathbf{k+q}})\delta(\varepsilon_{n,\mathbf{k}}-\varepsilon_{m,\mathbf{k+q}}+\hbar\omega_{\mathbf{q}\nu})\end{aligned} \tag{3}$$

In this work, we used the method of calculation of the electron-phonon matrix elements based on the density fuctional perturbation theory (DFPT)[18,19] and interpolation in the Wannier space.[16,20] using the EPW code.[16] Below, we present the technical details.

In this work, silicon is described within the LDA approximation, with a cutoff energy of 50 Ry and a 16x16x16 Γ-centered **k**-point grid. The theoretical lattice parameter of 10.2057 a.u. was used in all the calculations with the QUANTUM ESPRESSO package.[19]

The wannierization parameters for the Wannier90 code[21] were as follows: we used 10 initial Bloch functions, 8 Wannier functions with sp^3 initial projection (atom-centered), a window of 16.351 eV with a Frozen window of 6.211 eV and a 16x16x16 initial **k**-point grid. The disentanglement convergence with a 10^{-12} $\mathring{A}^2$ tolerance was reached in 302 iterations, whereas the spread minimization with a 10^{-10} $\mathring{A}^2$ tolerance was achieved in 600 iterations. The achieved spread for electrons was of 3.41 $\mathring{A}^2$.

For the interpolation of the electron-phonon matrix elements within the EPW code,[16] we used the above parameters and a 8x8x8 **q**-point grid.

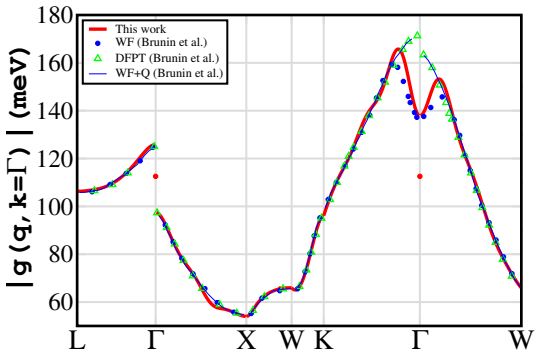

Figure 1. The comparison between the DFPT reference (green triangles), the results of Ref. 22 with and without quadrupolar interaction (blue line and blue dots, respectively), and our results (red line), for the electron-phonon matrix elements for the LO mode and for the initial electronic state which belongs to the the highest valence band with $\mathbf{k} = \Gamma$, and with $\mathbf{q}$ varying along the high-symmetry directions of the BZ.

Recently, it was shown in Refs. 22, 23 that the non-local quadrupolar interaction must be taken into account in order to achieve the correct interpolation of the electron-phonon coupling for the optical modes, even in non-polar materials such as Si.[22] In the present work, the quadrupolar interaction was not taken into account.

In Fig. 1, we show the comparison between the density functional perturbation theory (DFPT) reference, the results of Ref. 22 with and without the quadrupolar interaction, and our results, for the electron-phonon matrix elements for the longitudinal optical (LO) mode, for the initial electronic state which belongs to the the highest valence band of silicon with $\mathbf{k} = \Gamma$, and with the $\mathbf{q}$ vector varying along high-symmetry directions of the Brillouin zone (BZ).

As expected, our results are very close to the DFPT reference and to the results of Ref. 22, however a difference between the reference and our Wannier interpolation is visible around the Γ point in the $\Gamma - K$ and $\Gamma - W$ directions because of the absence of the quadrupolar interaction in our calculations. Indeed, without it, the interpolated electron-phonon matrix element tends to zero along some directions while it should tend to a finite value, as shown by the DFPT results. The portion of the BZ affected by this issue in non-polar materials such as silicon depends on the quality of the Wannier interpolation and on how dense is the $\mathbf{q}$-grid used for interpolation of the electron-phonon matrix elements.

Note that based on the comparison presented in Fig. 1, we do not expect the inclusion of the quadrupolar interaction to qualitatively change the conclusions of our work. Quantitatively, one might expect the role of optical phonons to be very slightly enhanced if the quadrupolar interaction was included. However, one must note that at high excess energy the electron-phonon scattering is dominated by intervalley phonons because of the very large density of final states, therefore the contribution of optical phonons around Γ point is expected to play a minor role.

3. RESULTS

While the total electron-phonon scattering rate involves the sum of emission and absorption probabilities over all possible final states, the rate of energy transfer to phonons involves, contrastingly, the difference between emission and absorption[3, 14, 17] (see eqns. 1-3).

In Fig. 2, we show the comparison between the total electron-phonon scattering rate (top panel) and energy transfer rate (bottom panel) for silicon as a function of electron excess energy, at 300 K and at 0 K. In Fig. 2, we have considered the initial electronic states along the $\Gamma - X$ direction in the Brillouin zone.

The upper panel of Fig. 2 demonstrates that the total electron-phonon scattering rate grows strongly with temperature, due to the growing populations of acoustic phonons. In contrast, as shown in the lower panel of Fig. 2, the energy transfer rate is found to be essentially independent of temperature, as the changes due to temperature in both emission and absorption contributions cancel each other.

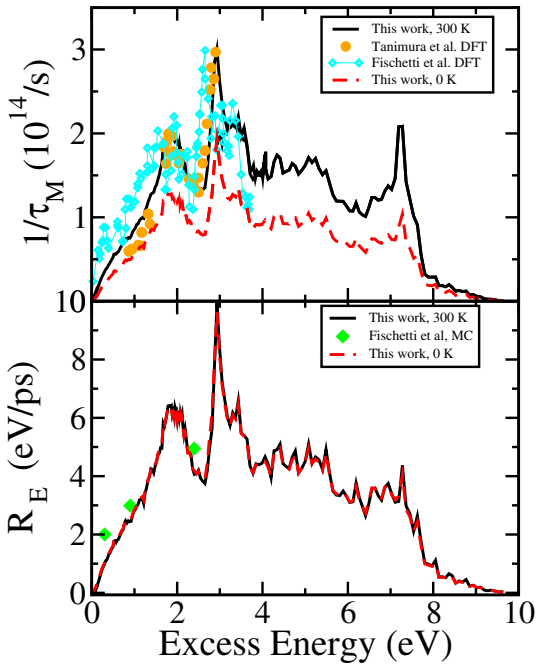

Figure 2. From our Ref. 15. Upper panel: Total electron-phonon scattering rate of hot electrons in silicon, at 300 K and 0 K. Initial state along the $\Gamma - X$ direction in the Brillouin zone. The theoretical DFT-based results from Tanimura *et al.*[12] and Fischetti *et al.*[24] at 300 K are also shown. Lower panel: Energy loss rate from electrons to phonons, at 300 K and 0 K. The results obtained by the Monte Carlo simulation method from Fischetti *et al.*[24] at 300 K is also shown (the correspondence between field and excess energy was taken from Ref. 25).

It must be noted that in the case of GaAs,[3] the energy transfer rate was found to decrease with growing temperature at low excess energies, and this inverse (with respect to the total electron-phonon scattering rate) temperature dependence of the energy transfer rate was found to disappear progressively with growing excess energy, the energy transfer rate becoming almost temperature independent at high excess energies. In contrast to GaAs, in silicon we find a negligible temperature dependence of the energy transfer rate at all excess energies. The difference between GaAs and Si probably comes from the difference in the topology of the conduction bands: whereas GaAs is a direct semiconductor with very narrow Γ valley, silicon is an indirect semiconductor and the lowest Δ valleys have large effective masses. Indeed, as explained in detail in Ref. 3, the main contribution to the energy loss rate is temperature-independent, whereas the temperature dependence comes from the additional contribution determined by the variations of the density of final electronic states available for electron-phonon transitions on the scale of the typical emitted/absorbed phonon energy. In the case of silicon, the variations of the density of final electronic states on the scale of the typical phonon energy are negligible due to large effective masses.

In Fig. 3 we analyse the contributions of the optical and acoustic modes to the total electron-phonon scattering rate and to the energy transfer rate. We note that we find the contribution of the acoustic phonons to the total scattering rate of hot electrons at 300 K to be comparable to that of the optical phonons when the initial states are considered along $\Gamma - X$ direction (Fig. 3, upper panel, solid lines). However, in contrast to room temperature results, at 0 K, the contribution of the optical phonons to the total scattering rate is found to be the largely dominant one (Fig. 3, upper panel, symbols). Therefore, the dominant role of the acoustic phonons in the total electron-phonon scattering rate of hot electrons in silicon at 300 K predicted by DFT is due to the increase of the populations of acoustic phonons at room temperature (Fig. 3, black curves). However, as already mentionned, it cancels out when the difference between emission and absorption is considered, as shown in the lower panel of Fig. 3. Indeed, as one can see in Fig. 3 (lower panel), the optical phonons are found by DFT to be the dominant channel of the energy relaxation of hot electrons in silicon at 300 K (as well as at 0 K).

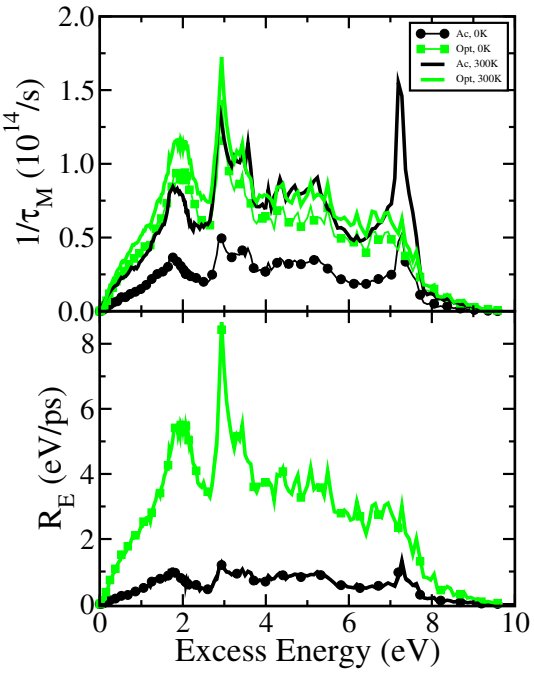

Figure 3. From our Ref. 15. Contributions of the acoustic and optical channels to the total electron-phonon scattering rate and to the energy loss rate of hot electrons in silicon, at 0 K and at 300 K. Initial state along the $\Gamma - X$ direction in the Brillouin zone. Upper panel: Acoustic and optical phonon contributions to the total electron-phonon scattering rate. Thick solid lines: acoustic (black) and optical (green) contributions to the total electron-phonon scattering rate at 300 K. Symbols with thin lines: acoustic (black circles) and optical (green squares) contributions to the total electron-phonon scattering rate at 0 K. Lower panel: Acoustic and optical phonon contributions to the energy loss rate. Thick solid lines: acoustic (black) and optical (green) contributions to the energy loss rate at 300 K. Symbols with thin lines: acoustic (black circles) and optical (green squares) contributions to the energy loss rate at 0 K.

4. CONCLUSION

In conclusion, we have shown that, in contrast to the total scattering rate, the rate of energy transfer from highly excited electrons to phonons has a negligible temperature dependence in silicon. Moreover, we have demonstrated, on the basis of DFT results, that the dominant electron-phonon scattering channels may differ for the total electron-phonon scattering rate and for the energy loss rate. This fact, pointed out previously, e.g., in Ref. 14, turns out to play an important role in silicon at room temperature.[15]

ACKNOWLEDGMENTS

This work was financed by CEA ANCRE program (project Thermoint). The support from Labex Nanosaclay, ANR-10-LABX-0035 (Flagship project MaCaCQu) and from ANR via ANR-21-CE50-0008 (project Placho) is also gratefully acknowledged.

The access to high performance computing resources was granted by the French HPC centers GENCI-IDRIS, GENCI-CINES and GENCI-TGCC (Project 2210) and by the cole Polytechnique through the 3L-HPC project. Financial support from the DIM SIRTEQ (rgion le de France) is also gratefully acknowledged.

The calculations were performed using Quantum ESPRESSO,[19] EPW[16] and Wannier90[21] packages.

R. S. also gratefully acknowledges the support and kind assistance from Prof. Priya Johari (Shiv Nadar University, India).

REFERENCES

[1] Bernardi, M., "First-principles dynamics of electrons and phonons," *Eur. Phys. J. B* **89**, 15 (2016).

[2] Giustino, F., "Electron-phonon interactions from first principles," *Rev. Mod. Phys.* **89**, 015003 (2017). And refererences herein.

[3] Sjakste, J., Vast, N., Barbarino, G., Calandra, M., Mauri, F., Kanasaki, J., Tanimura, H., and Tanimura, K., "Energy relaxation mechanism of hot-electron ensembles in GaAs: Theoretical and experimental study of its temperature dependence," *Phys. Rev. B* **97**, 064302 (2018).

[4] Papalazarou, E., Faure, J., Mauchain, J., Marsi, M., Taleb-Ibrahimi, A., Reshetnyak, I., van Roekeghem, A., Timrov, I., Vast, N., Arnaud, B., and Perfetti, L., "Coherent phonon coupling to individual Bloch states in photoexcited bismuth," *Phys. Rev. Let.* **108**, 256808 (2012).

[5] Kanasaki, J., Tanimura, H., and Tanimura, K., "Imaging energy-, momentum-, and time-resolved distributions of photoinjected hot electrons in GaAs," *Phys. Rev. Lett.* **113**, 237401 (2014).

[6] Tanimura, H., Kanasaki, J., Tanimura, K., Sjakste, J., Vast, N., Calandra, M., and Mauri, F., "Formation of hot-electron ensembles quasiequilibrated in momentum space by ultrafast momentum scattering of highly excited hot electrons photoinjected into the Γ valley of GaAs," *Phys. Rev. B* **93**, 161203(R) (2016).

[7] Zürch, M., Chang, H.-T., Borja, L. J., Kraus, P. M., Cushing, S. K., Gandman, A., Kaplan, C. J., Oh, M. H., Prell, J. S., Prendergast, D., Pemmaraju, C. D., Neumark, D. M., and Leone, S. R., "Direct and simultaneous observation of ultrafast electron and hole dynamics in germanium," *Nat. Commun.* **8**, 15734 (2017).

[8] Chen, Z., Sjakste, J., Dong, J., Taleb-Ibrahimi, A., Rueff, J.-P., Shukla, A., Peretti, J., Papalazarou, E., Marino, M., and Perfetti, L., "Ultrafast dynamics of hot carriers in a quasi-two-dimensional electron gas on inse," *PNAS* **117**, 21962–21967 (2020).

[9] Wörle, M., Holleitner, A. W., Kienberger, R., and Iglev, H., "Ultrafast hot carrier relaxation in silicon monitored by phase-resolved transient absorption spectroscopy," *Phys. Rev. B* **104**, L041201 (2021).

[10] Bernardi, M., Vigil-Fowler, D., Lischner, J., Neaton, J. B., and Louie, S. G., "Ab initio study of hot carriers in the first picosecond after sunlight absorption in silicon," *Phys. Rev. Lett.* **112**, 257402 (2014).

[11] Sjakste, J., Tanimura, K., Barbarino, G., Perfetti, L., and Vast, N., "Hot electron relaxation dynamics in semiconductors: assessing the strength of the electron-phonon coupling from the theoretical and experimental viewpoints," *J. Phys.: Condens. Matter* **30**, 353001 (2018).

[12] Tanimura, H., Kanasaki, J., Tanimura, K., Sjakste, J., and Vast, N., "Ultrafast relaxation dynamics of highly excited hot electrons in silicon," *Phys. Rev. B* **100**, 035201 (2019).

[13] Chen, Z., Giorgetti, C., Sjakste, J., Cabouat, R., Veniard, V., Zhang, Z., Taleb-Ibrahimi, A., Papalazarou, E., Marsi, M., Shukla, A., Peretti, J., and Perfetti, L., "Ultrafast electron dynamics reveal the high potential of InSe for hot-carrier optoelectronics," *Phys. Rev. B* **97**, 241201(R) (2018).

[14] Ahmad, S., Daga, O., and Khokle, W., "Energy and momentum loss rates for hot electrons in silicon.," *Phys. Stat. Sol.* **40**, 631 (1970).

[15] Sen, R., Vast, N., and Sjakste, J., "Hot electron relaxation and energy loss rate in silicon: Temperature dependence and main scattering channels," *Appl. Phys. Lett.* **120**, 082101 (2022).

[16] Ponce, S., Margine, E. R., Verdi, C., and Giustino, F., "EPW: Electron-phonon coupling, transport and superconducting properties using maximally localized Wannier functions.," *Comp. Phys. Comm.* **209**, 116 (2016).

[17] Allen, P., "Theory of thermal relaxation of electrons in metals," *Phys. Rev. Lett.* **59**, 1460 (1987).

[18] Baroni, S., de Gironcoli, S., Corso, A. D., and Giannozzi, P., "Phonons and related crystal properties from density-functional perturbation theory," *Rev. Mod. Phys.* **73**, 515 (2001).

[19] Giannozzi, P., Andreussi, O., Brumme, T., Bunau, O., Nardelli, M. B., Calandra, M., Car, R., Cavazzoni, C., Ceresoli, D., Cococcioni, M., Colonna, N., Carnimeo, I., Corso, A. D., de Gironcoli, S., Delugas, P., Ferretti, R. A. D. J. A., Floris, A., Fratesi, G., Fugallo, G., Gebauer, R., Gerstmann, U., Giustino, F., Gorni, T., Jia, J., Kawamura, M., Ko, H.-Y., Kokalj, A., Küçükbenli, E., Lazzeri, M., Marsili, M., Marzari, N., Mauri, F., Nguyen, N. L., Nguyen, H.-V., de-la Roza, A. O., Paulatto, L., Poncé, S., Rocca, D., Sabatini, R., Santra, B., Schlipf, M., Seitsonen, A. P., Smogunov, A., Timrov, I., Thonhauser, T., Umari, P., Vast, N., Wu, X., and Baroni, S., "Advanced capabilities for materials modelling with Quantum ESPRESSO," *J. Phys.: Condens. Matter* **29**, 465901 (2017).

[20] Calandra, M., Profeta, G., and Mauri, F., "Adiabatic and nonadiabatic phonon dispersion in a Wannier approach," *Phys. Rev. B* **82**, 165111 (2010).

[21] Pizzi, G., Vitale, V., Arita, R., Blgel, S., Freimuth, F., Géranton, G., Gibertini, M., Gresch, D., Johnson, C., Koretsune, T., Ibañez-Azpiroz, J., Lee, H., Lihm, J. M., Marchand, D., Marrazzo, A., Mokrousov, Y., Mustafa, J. I., Nohara, Y., Nomura, Y., Paulatto, L., Poncé, S., Ponweiser, T., Qiao, J., Thle, F., Tsirkin, S. S., Wierzbowska, M., Marzari, N., Vanderbilt, D., Souza, I., Mostofi, A. A., and Yates, J. R., "Wannier90 as a community code: new features and applications," *J. Phys.: Condens. Matter* **32**, 165902 (2020).

[22] Brunin, G., Miranda, H. P. C., Giantomassi, M., Royo, M., Stengel, M., Verstraete, M. J., Gonze, X., Rignanese, G.-M., and Hautier, G., "Electron-phonon beyond Frhlich: Dynamical quadrupoles in polar and covalent solids," *Phys. Rev. Lett.* **125**, 136601 (2020).

[23] Jhalani, V. A., Zhou, J.-J., Park, J., Dreyer, C. E., and Bernardi, M., "Piezoelectric electron-phonon interaction from ab initio dynamical quadrupoles: Impact on charge transport in wurtzite GaN," *Phys. Rev. Lett.* **125**, 136602 (2020).

[24] Fischetti, M. V., Yoder, P., Khatami, M., Gaddemane, G., and de Put, L. V., "Hot electrons in Si lose energy to optical phonons: Truth or myth?," *Appl. Phys. Lett.* **114**, 222104 (2019).

[25] Fischetti, M. V. and Laux, S. E., "Monte Carlo analysis of electron transport in small semiconductor devices including band-structure and space-charge effects," *Phys. Rev. B* **38**, 9721 (1988).